

## Research Article

# An Alternative *In Vivo* Model to Evaluate Pluripotency of Patient-Specific hiPSCs

Josefin Weber<sup>#</sup>, Marbod Weber<sup>#</sup>, Heidrun Steinle, Christian Schlensak, Hans Peter Wendel and Meltem Avci-Adali

University Hospital Tuebingen, Department of Thoracic and Cardiovascular Surgery, Tuebingen, Germany

### Abstract

The generation of autologous human induced pluripotent stem cells (hiPSCs) from a patient's somatic cells and the subsequent differentiation of these cells into desired cell types offer innovative treatment options for tissue regeneration. The hiPSCs obtained are usually implanted in immunodeficient mice, and teratoma formation is analyzed after 4 to 6 weeks to assess the cells' pluripotency. In this study, an alternative *in vivo* model based on chicken egg chorioallantoic membrane (CAM) was established to analyze the pluripotency of newly created hiPSCs.  $0.5$ ,  $1$ ,  $2$ ,  $4 \times 10^6$  hiPSCs generated from urine-derived renal epithelial cells were seeded on CAM and incubated for 9 days. Teratoma formation was detected in 70% of eggs inoculated with  $2 \times 10^6$  hiPSCs and in 100% of eggs inoculated with  $4 \times 10^6$  hiPSCs. All teratomas exhibited vascular structures. The robustness of the CAM model was confirmed using two additional hiPSC lines derived from human fibroblasts (NuFFs) or jaw periosteal cells. The presence of all three germ layers within the teratomas was successfully verified by histochemical and immunofluorescence staining and gene expression analysis of germ layer-specific markers. Urine-derived renal epithelial cells were used as negative control and showed no teratoma formation. The CAM-based *in vivo* model provides an optimal *in vivo* test environment for the pluripotency evaluation of newly generated hiPSC lines. This simple, fast, inexpensive and reproducible method reduces the suffering of animals and thus implements the principles of the 3Rs (replacement, reduction, and refinement).

## 1 Introduction

The groundbreaking discovery of the reprogrammability of somatic cells into human induced pluripotent stem cells (hiPSCs) opened up new opportunities in the field of tissue engineering and the development of personalized cell therapies. Since hiPSCs are derived from patient's somatic cells, their generation and use avoid ethical concerns related to embryonic stem cells. Thus, hiPSCs are a promising cell source to generate patient-specific cell types. Yamanaka and colleagues first reprogrammed murine fibroblasts into iPSCs (Takahashi and Yamanaka, 2006), and shortly thereafter reprogramming was also demonstrated in human fibroblasts using retroviral vectors encoding four transcription factors, Klf4, c-Myc, Oct4 and Sox2 (Takahashi et al., 2007). However, retroviral vectors are inserted into the host genome, and this is associated with a significant risk of insertional mutagenesis, incomplete transgene silencing or reactivation, and residual expression of reprogramming factors, which can lead to

tumor development (Cieřlar-Pobuda et al., 2017). Therefore, to prevent genetic alterations in hiPSCs for later clinical applications, several non-genome integrating approaches have been developed (Kaji et al., 2009; Yu et al., 2009; Warren et al., 2010). Especially, synthetic messenger RNA-based reprogramming methods using synthetic messenger RNA (mRNA) or self-replicating RNA (srRNA) are promising (Steinle et al., 2017, 2019a). After the exogenous delivery of reprogramming factor-encoding RNAs into somatic cells, desired reprogramming factors are expressed under physiological conditions by the cellular translational machinery until the cells are reprogrammed. In comparison to plasmid DNA, synthetic mRNAs or srRNAs do not need to enter the cell nucleus. This allows the expression of desired proteins in dividing and non-dividing cells and results in an immediate translation of delivered mRNA or srRNA in the cytosol. Since these RNAs are not integrated into the genome, the risk of insertional mutagenesis can be eliminated (Rabinovich and Weissman, 2013).

<sup>#</sup> contributed equally

Received May 22, 2020; Accepted January 20, 2021;  
Epub January 25, 2021; © The Authors, 2021.

ALTEX 38(3), 442-450. doi:10.14573/altex.2005221

Correspondence: Meltem Avci-Adali, PhD  
Department of Thoracic and Cardiovascular Surgery, University Hospital Tuebingen  
Calwerstr. 7/1, 72076 Tuebingen, Germany  
(meltem.avci-adali@uni-tuebingen.de)

This is an Open Access article distributed under the terms of the Creative Commons Attribution 4.0 International license (<http://creativecommons.org/licenses/by/4.0/>), which permits unrestricted use, distribution and reproduction in any medium, provided the original work is appropriately cited.

After the successful generation of hiPSC lines, a detailed characterization of the cells is essential. In addition to the exclusion of genetic abnormalities and the expression of proteins associated with stem cell properties, the confirmation of pluripotency is required. To confirm the pluripotency of newly generated hiPSC lines, their differentiation into three germ layers is analyzed by subcutaneous or intramuscular injection of hiPSCs in immunodeficient mice (DeBord et al., 2018; Nelakanti et al., 2015). Animals are monitored for approximately 6 weeks and sacrificed to explant the teratoma before it is larger than 1 cm<sup>3</sup>. Because of its tumor-like growth, it can cause the animals pain and suffering and therefore raises ethical concerns (Buta et al., 2013). In addition, keeping immunodeficient mice is time-consuming and expensive.

In recent years, the chorioallantoic membrane (CAM) assay was applied to investigate angiogenesis (Steinle et al., 2018; Naik et al., 2018), tumorigenesis (Li et al., 2015; Dexter et al., 1983; Duropt et al., 2012; Rovithi et al., 2017), bone and cartilage generation (Moreno-Jimenez et al., 2016), and irritant potential of chemicals (Gilleron et al., 1996; Ying et al., 2010). CAM is formed by the fusion of the mesodermal layer of the allantois with the mesodermal layer of the chorion by the third day of development of the chicken embryo (Kunz et al., 2019; Dohle et al., 2009). The highly vascularized CAM mimics a perfect environment for cell transplantation, and it can maintain engrafted cells (Deryugina and Quigley, 2008). Furthermore, the CAM assay provides a highly reproducible, cost-effective, immunodeficient, and non-innervated extra-embryonic test environment (Kunz et al., 2019; Kunzi-Rapp et al., 2001) and can be used to implement the 3R principles (reduction, replacement, and refinement) (Petrovova et al., 2019). An ethical advantage of the CAM assay is that the CAM itself is not innervated, allowing the growth of xenografts without pain or impairment of the embryo (Kunz et al., 2019). Furthermore, the lack of nociception in chicken embryos due to incomplete neuronal differentiation until day 14 of the gestation period makes the model a favorable alternative to rodent models (Buhr et al., 2020). Therefore, in some countries, ethical approval is not required for CAM assays with chicken embryos until 14 days of development. In other countries, the chicken embryo is not considered an independent living animal until day 17 or until hatching (Winter et al., 2020), so ethical approval for animal experiments is not required. Thus, depending on the country, the legal requirements should be followed and, if necessary, the approval of an ethics committee for animal experiments should be obtained.

In this study, we describe the applicability of a CAM assay-based *in vivo* model as an alternative to conventional rodent models for analyzing the pluripotency of patient-specific hiPSCs by spontaneous teratoma formation.

## 2 Materials and methods

### *Cultivation of hiPSCs*

Footprint-free hiPSCs were generated by reprogramming human renal epithelial cells (RECs) isolated from 100–200 mL urine of healthy human donors using VEE-OKSiM-GFP srRNA encoding OCT4, KLF4, SOX2, cMYC, and GFP. Transfection and

reprogramming were performed according to our recent study (Steinle et al., 2019b). The obtained hiPSCs were cultivated on T25 culture flasks coated with 0.5 mg/cm<sup>2</sup> vitronectin (Thermo Fisher Scientific, Waltham, MA, USA) in E8 stem cell medium (Essential 8, Thermo Fisher Scientific) at 37°C and 5% CO<sub>2</sub>. After reaching 70% confluence, hiPSCs were washed once with Dulbecco's phosphate-buffered saline (DPBS) (Thermo Fisher Scientific) and incubated for 5 min at 37°C with DPBS containing 0.5 mM ethylenediaminetetraacetic acid (EDTA, Sigma-Aldrich, Steinheim, Germany). After detachment, cells were suspended in E8 medium containing 10 µM ROCK inhibitor Y-27632 (Enzo Life Sciences, Lausen, Switzerland) and passaged at a 1:10 split ratio into a new vitronectin-coated T25 culture flask. hiPSCs were cultivated at 37°C and 5% CO<sub>2</sub> (normoxia). After 24 h, the medium was changed to E8 medium without ROCK inhibitor Y-27632, and daily medium changes were performed.

### *Cultivation of RECs*

RECs were isolated as described in our previous study (Steinle et al., 2019b) and cultivated at 37°C with 5% CO<sub>2</sub> in 0.1% gelatin-coated 12-well plates with proliferation medium consisting of 50% renal epithelial (RE) basal medium with REGM Bullet Kit supplements (Lonza, Basel, Switzerland) and 50% mesenchymal cell proliferation medium (DMEM high glucose supplemented with 10% fetal bovine serum (FBS), 1x GlutaMax, 1x MEM (minimum essential medium) non-essential amino acids (NEAA), 50 mg/mL gentamicin, 250 mg/mL amphotericin B, 5 ng/mL basic fibroblast growth factor (bFGF), 5 ng/mL platelet-derived growth factor (PDGF)-AB, and 5 ng/mL epidermal growth factor (EGF). Cell culture reagents were obtained from Thermo Fisher Scientific, and recombinant human growth factors were acquired from Peprotech (Hamburg, Germany). The medium was changed every three days. When reaching 80% confluency, RECs were passaged using 0.04% trypsin/0.03% EDTA. The reaction was stopped with trypsin-neutralizing solution (TNS; 0.05% trypsin inhibitor in 0.1% BSA, PromoCell, Heidelberg, Germany). Then, cells were centrifuged for 5 min at 300 x g and seeded on 0.1% gelatin-coated (Sigma-Aldrich) T75 cell culture flasks.

### *Chorioallantoic membrane (CAM) assay*

Fertilized chicken eggs of the Lohmann White x White Rock breed chicken were obtained from a breeding facility (Matthias Sittig, Buchholz, Germany). Feathers, dirt and excrement were removed from the eggshells by wiping with a wet tissue. The eggs were placed in an egg incubator (Heka-Brutgeräte, Rietberg-Varensell, Germany) and incubated at 37°C and 60% relative humidity (Day 0). The eggs were completely rotated twice a day. At day 3 after fertilization, an 18G needle was inserted at the tip of the egg without harming the yolk, and 2–3 mL albumen was removed to lower the level of the CAM. A semi-permeable adhesive tape, Suprasorb F (Lohmann & Rauscher, Rengsdorf, Germany) was fixed on the eggshell. Then, under a sterile bench, using sterile surgical scissors, a circular opening (Ø 1–1.5 cm) was cut into the eggshell without damaging the CAM. Unfertilized eggs without a beating heart or without vasculature were discarded. Afterwards, the window of the eggshell of viable eggs was



closed with the adhesive tape to prevent dehydration and to minimize the risk of contamination. Subsequently, eggs were incubated without rotation at 37°C and 75% relative humidity. On day 7, the semi-permeable adhesive tape covering the circular opening was carefully opened with sterile scissors and the development of the eggs was analyzed. Insufficiently developed or contaminated eggs without clearly visible vasculature and movement of the embryo were removed. Sterile silicone sealing rings of cryovials with an inner diameter of 0.85 cm (neoLab, Leonberg, Germany) were carefully placed onto the CAM. 0.5, 1, 2, or 4 × 10<sup>6</sup> hiPSCs (passage 11) suspended in 50 µL cell culture medium and mixed with 50 µL Matrigel (hECS qualified, Corning, NY, USA) were applied into the silicone ring. As a control, 1 × 10<sup>6</sup> RECs were applied onto the CAM. After the application, the opening in the eggshell was sealed with the adhesive tape again and further incubated at 38°C and 80% relative humidity. On day 16, the CAMs including the generated teratoma were excised around the silicone ring and fixed overnight at 4°C with 4% paraformaldehyde (PFA, Merck, Darmstadt, Germany) for further analysis.

To verify the robustness of the CAM model, 2 × 10<sup>6</sup> hiPSCs generated from newborn human foreskin fibroblasts (NuFFs, Amsbio, Milton Park, UK) or human jaw periosteal cells (obtained from Prof. Dr Dorothea Alexander-Friedrich, Department of Oral and Maxillofacial Surgery, University Hospital Tübingen) using srRNA were also applied onto CAM, and the generated teratomas were analyzed.

#### *Paraffin embedding and histochemical evaluation of teratomas*

The PFA-fixed teratomas and CAMs seeded with RECs as negative controls were washed with DPBS, dehydrated using an ascending ethanol series (50%, 70%, 80%, 90%, 99%), and embedded in paraffin for sectioning. Using a microtome (MICROM GmbH, Walldorf, Germany), 5 µm sections were cut from paraffin-embedded tissues. Sections were placed on SuperFrost microscope slides (R. Langenbrinck GmbH, Emmendingen). The sections were then deparaffinized and rehydrated with xylene, a descending ethanol series (100%, 80%, 70%, 60%), and deionized water. Afterwards, the sections were stained with hematoxylin and eosin (H&E) (Morphisto, Frankfurt, Germany). In the next step, sections were dehydrated using an ascending ethanol series (60%, 70%, 80%, 100%), and xylene. Finally, the sections were covered with glass coverslips. The teratoma structures were microscopically analyzed regarding the presence of tissue-specific structures.

To prove the presence of cells from all three germ layers, immunohistochemical staining was performed using an automated immunostainer (Ventana Medical Systems, Inc., Arizona, USA) and specific antibodies against early cell types of three germ layers according to the company's protocols with slight modifications. Monoclonal mouse anti-human CD34 antibody (Dako, Agilent Technologies, Santa Clara, USA) was used to show the presence of mesoderm tissue. CD34 is a marker for hematopoietic stem cells and endothelial progenitor cells. Monoclonal mouse anti-human SALL4 antibody (M03, clone 6E3, (Abnova, Taipeh, Taiwan) was used to detect endoderm tissue. The presence of ectodermal tissue was assessed using the monoclonal mouse anti-human vimentin (V9) (ROCHE, Basel,

Switzerland) antibody, which is a neural and pancreatic progenitor cell marker. All antibodies were visualized by the automated immunostainer using DAB (deaminobenzidine). Counterstaining was performed using hematoxylin. Images were taken using an Axiovert135 microscope (Carl Zeiss, Oberkochen, Germany) and EOS Utility software (Canon, Tokyo, Japan).

#### *Cryosectioning and immunofluorescence staining of teratomas*

The PFA-fixed teratomas were washed in DPBS and then dehydrated at RT by sucrose (Saccharose, Sigma-Aldrich) solutions of increasing concentrations (10%, 15%, 20%) for 15 min each. Teratomas were then transferred into Tissue-Tek Cryomolds (Sakura Finetek Germany GmbH, Staufen im Breisgau, Germany), embedded in Tissue-Tek (Sakura Finetek Germany GmbH), and stored at -80°C. The frozen block was sectioned at 18 µm using a cryomicrotome (Leica Biosystems Nussloch GmbH, Nußloch, Germany). After overnight drying at RT, the sections were immunostained.

To perform immunofluorescence staining, the teratoma sections were washed with DPBS and blocked with 4% BSA in DPBS for 1 h at RT. Sections were then incubated for 1 h at RT with fluorescently labeled antibodies in DPBS with 2% BSA or in DPBS with 2% BSA and Triton X-100 (Sigma-Aldrich) for intracellular staining. After washing, the coverslips were mounted using Fluoroshield mounting medium with DAPI (Abcam, Cambridge, UK). Alexa Fluor® 488-mouse anti-human β-tubulin (BD Biosciences, Franklin Lakes, USA), PE-mouse anti-human CD31, and PE-mouse anti-human CXCR4 (both from Miltenyi Biotec, Bergisch Gladbach, Germany) antibodies were used to detect the three different germ layers. Staining with the respective isotypes was performed as control.

#### *qRT-PCR analysis*

RNA was isolated from the explanted teratomas generated from 2 × 10<sup>6</sup> hiPSCs or hiPSCs cultivated in cell culture plates (control) using the Aurum™ Total RNA Mini Kit (Bio-Rad, Munich, Germany). 300 ng RNA was reverse transcribed into complementary DNA (cDNA) using the iScript kit (Bio-Rad). The primers used for the specific amplification of transcripts, ordered from Eurofins (Luxembourg, Luxembourg) or ELLA Biotech (Martinsried, Germany), are listed in Table 1. They were used at a final concentration of 300 nM. Real-time qRT-PCR reactions were performed in a CFX Connect Real-Time PCR Detection System (Bio-Rad) using IQ SYBR Green Supermix (Bio-Rad). Expression of the constitutively expressed gene GAPDH (glyceraldehyde 3-phosphate dehydrogenase) was used as an internal control for the amount of RNA input. Primers were designed by using the Primer-Blast tool from NCBI (Ye et al., 2012). Melting temperatures and self-complementarities were checked using the Oligonucleotide Properties Calculator from Northwestern University Medical School (Kibbe, 2007).

The qRT-PCR amplification of cDNA was performed under the following conditions: 3 min at 95°C for one cycle, followed by 40 cycles of 95°C for 15 s, 60°C for 30 s, and 72°C for 10 s. After 40 cycles, melt curve analyses were performed to detect the specific amplification of transcripts. The qRT-PCR reactions

**Tab. 1: List of primer sequences used for qRT-PCR analysis**

Gene	Germ layer	Forward primer 5' - 3'	Reverse primer 5' - 3'
GAPDH	-	TCAACAGCGACACCCACTCC	TGAGGTCCACCACCCTGTTG
CD31	Mesoderm	GAACGGAAGGCTCCCTTGA	AGGGCAGGTTCAATAAAGTGTC
CD34		GATTGCACTGGTCACCTCGG	TCCGTGTAATAAGGGTCTTCGC
$\alpha$ SMA		GAGGGAAGGTCCTAACAGCC	TAGTCCCGGGGATAGGCAAA
FOXA2	Endoderm	TGCACTCGGCTTCCAGTATG	CGTGTTTCATGCCGTTTCATCC
AFP		AAATGCGTTTCTCGTTGCTT	GAGTTGGCAACAAGTGGCTG
Pax6	Ectoderm	CTGAGGAATCAGAGAAGACAGGC	ATGGAGCCAGATGTGAAGGAGG
Sox1		AATACTGGAGACGAACGCCG	AACCCAAGTCTGGTGTGTCAGC

GAPDH, glyceraldehyde-3-phosphate dehydrogenase;  $\alpha$ SMA, alpha-smooth muscle actin; FOXA2, forkhead box protein A2; AFP, alpha-fetoprotein; Pax6, paired box gene 6; Sox1, sex determining region Y-box 1a

were run in triplicates with a total volume of 15  $\mu$ L per well. Levels of mRNA for each gene were normalized to GAPDH. The results are shown relative to control mRNA levels.

### 3 Results

#### 3.1 Analysis of teratoma formation upon application of hiPSCs onto CAM

To analyze the teratoma formation of newly generated hiPSCs, a CAM-based assay was established (Fig. 1A). The viability of embryos was evaluated using 176 viable eggs. After the opening of eggs on day 3 and incubating the eggs until day 7, 15 embryos died, which corresponds to a survival rate of 91%. After 16 days, 63% of the initial embryos were still viable (Fig. 1B).

Using a total of 33 eggs, the formation of teratomas was analyzed by seeding different numbers of hiPSCs on CAM. Teratoma formation was analyzed 9 days after the inoculation of CAM with 0.5, 1, 2, or 4  $\times 10^6$  hiPSCs (Fig. 1C). Teratomas were formed in 30% (3/10) of the eggs after the application of 0.5  $\times 10^6$  hiPSCs, 50% (5/10) after the application of 1  $\times 10^6$  hiPSCs, and 70% (7/10) after the application of 2  $\times 10^6$  hiPSCs. The application of 4  $\times 10^6$  hiPSCs resulted in the formation of teratomas in 100% (3/3) of the eggs (Fig. S1<sup>1</sup>).

#### 3.2 Analysis of teratoma size, tissue structures, and vascularization

On the 16<sup>th</sup> day of incubation, the hiPSC-derived teratomas were explanted (Fig. 2A and Fig. S1B<sup>1</sup>). The H&E staining of CAMs seeded with 0.5, 1, 2  $\times 10^6$  (Fig. 2B) or 4  $\times 10^6$  hiPSCs (Fig. S1D<sup>1</sup>) showed that the teratomas contained different types of tissues. The seeding of 1  $\times 10^6$  RECs onto the CAM showed no teratoma formation (Fig. 2B, control). Measuring the size of the teratomas (Fig. 2A,C) revealed that the seeding of 2  $\times 10^6$  hiPSCs on CAM

led to an increased teratoma size ( $24.47 \pm 11.71$  mm<sup>2</sup>) compared to the seeding of 1  $\times 10^6$  ( $12.79 \pm 1.91$  mm<sup>2</sup>) or 0.5  $\times 10^6$  hiPSCs ( $12.5 \pm 0.69$  mm<sup>2</sup>) (Fig. 2C). Histological examinations showed the formation of vascular structures within the teratomas, which enable the blood supply to the cells (Fig. 2D).

#### 3.3 Analysis of the tri-lineage differentiation of the hiPSCs

H&E staining of the explanted teratomas that were generated from 2  $\times 10^6$  hiPSCs revealed their tri-lineage differentiation (Fig. 3). Differentiation into mesodermal tissue was demonstrated by the presence of bone-like structures (Fig. 3A I) and differentiation into endodermal tissue was shown by the detection of the primitive gut-like epithelium (Fig. 3A II). The presence of squamous epithelial tissue (Fig. 3A III) showed the differentiation of hiPSCs into ectoderm tissue.

Immunohistochemical analyses demonstrated the expression of the mesodermal marker CD34 (Fig. 3B I), endodermal marker SALL4 (Fig. 3B II), and the ectodermal marker vimentin (Fig. 3B III) associated with the respective morphological structures. The antibodies showed no binding to tissue sections of CAMs that were seeded with RECs (Fig. S2A<sup>1</sup>).

The immunofluorescence analyses of cryosections with specific antibodies revealed a strong expression of CD31 within the mesodermal tissue structures (Fig. 3C I), CXCR4 within endodermal tissue (Fig. 3C II), and  $\beta$ -tubulin within ectodermal structures (Fig. 3C III). Isotype controls showed no binding (Fig. S2B<sup>1</sup>). Furthermore, the immunofluorescence analyses of CAMs seeded with RECs showed no binding to CAM (Fig. S2C<sup>1</sup>).

Using qRT-PCR, increased expression of mesoderm (CD31, CD34, and SMA), endoderm (FOXA2 and AFP) and ectoderm (SOX1 and PAX6) markers was detected on CAMs seeded with 2  $\times 10^6$  hiPSCs and incubated for 16 days compared to hiPSCs cultivated in cell culture flasks with E8 medium (Fig. 3D).

<sup>1</sup> doi:10.14573/altex.2005221s



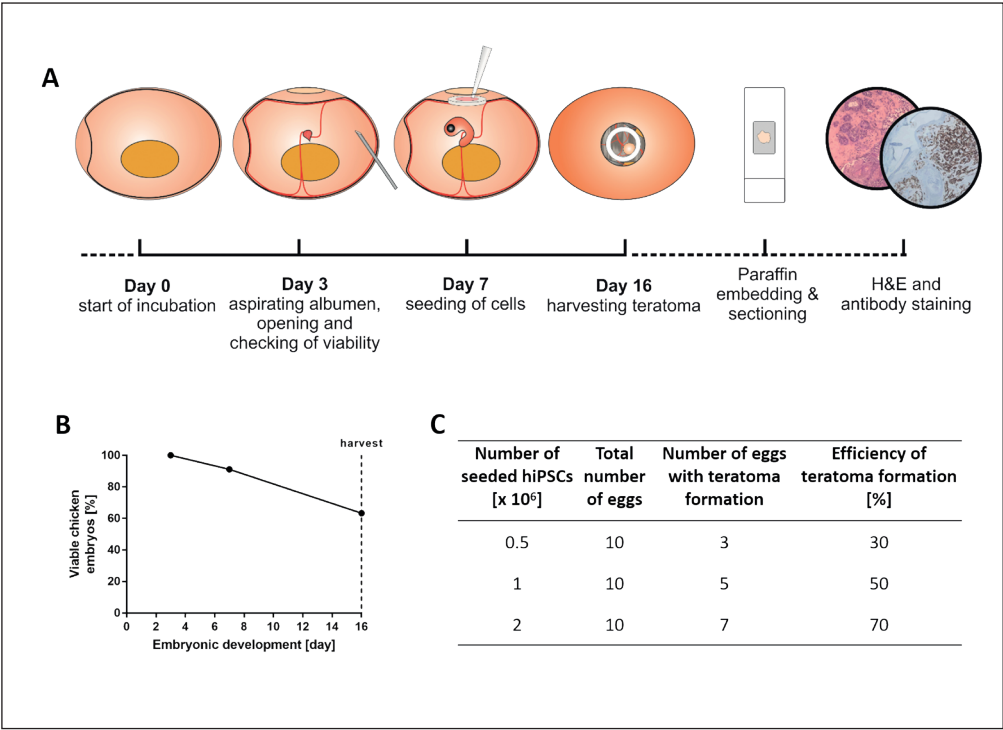


**Fig. 1: Evaluation of teratoma formation after the seeding of hiPSCs on CAM**

(A) Schematic representation of the CAM-based assay to evaluate teratoma formation. The teratoma formation assay was completed within 16 days after the start of incubation of the eggs. Subsequently, teratomas were embedded, sectioned, and histologically analyzed. (B) Survival rate of chicken embryos in the CAM assay ( $n = 176$ ). (C) Efficiency of teratoma formation depending on the inoculated hiPSC numbers on CAM.

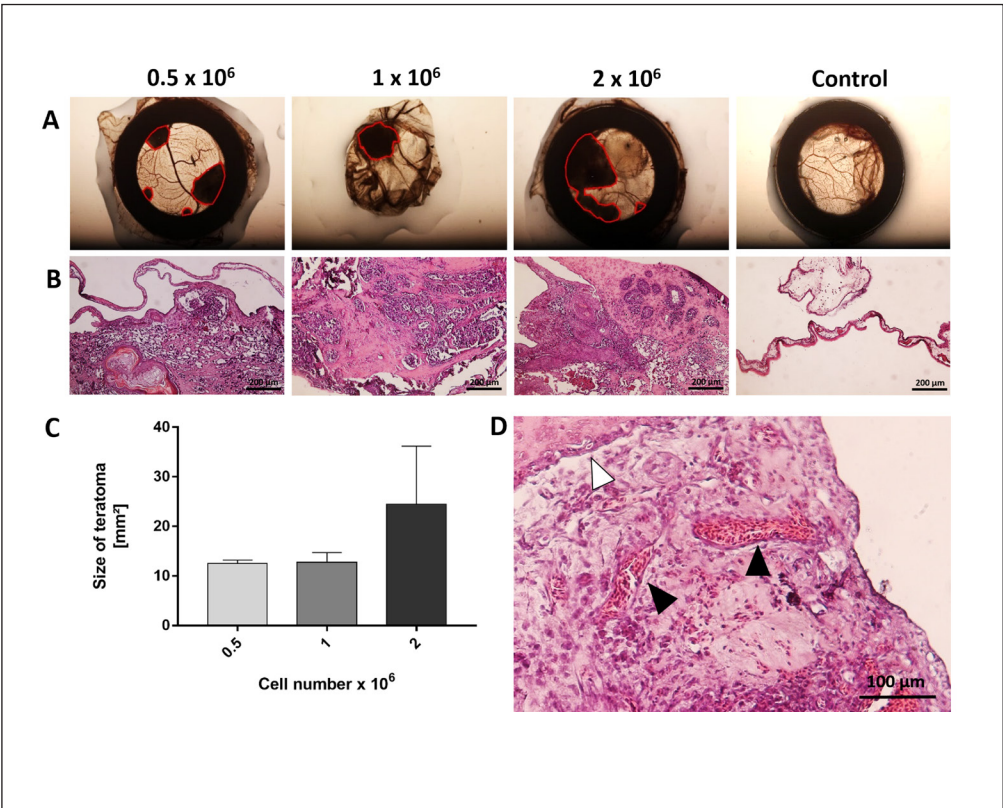


**Fig. 2: Analysis of teratoma size, tissue structures and vascularization**

(A) Pictures of excised CAM with formed teratomas after the seeding of 0.5, 1, or 2  $\times 10^6$  hiPSCs on CAM. As a control, 1  $\times 10^6$  RECs were seeded. Teratomas are encircled in red. (B) H&E-stained sections of the teratomas or CAM. (C) The size of the generated teratomas was determined by area calculation (red encircled area in A). (D) H&E staining of a teratoma section showing vascular structures (black arrows) inside a teratoma generated from 2  $\times 10^6$  hiPSCs. The white arrow shows the CAM. Images are representative of  $n = 10$  eggs.

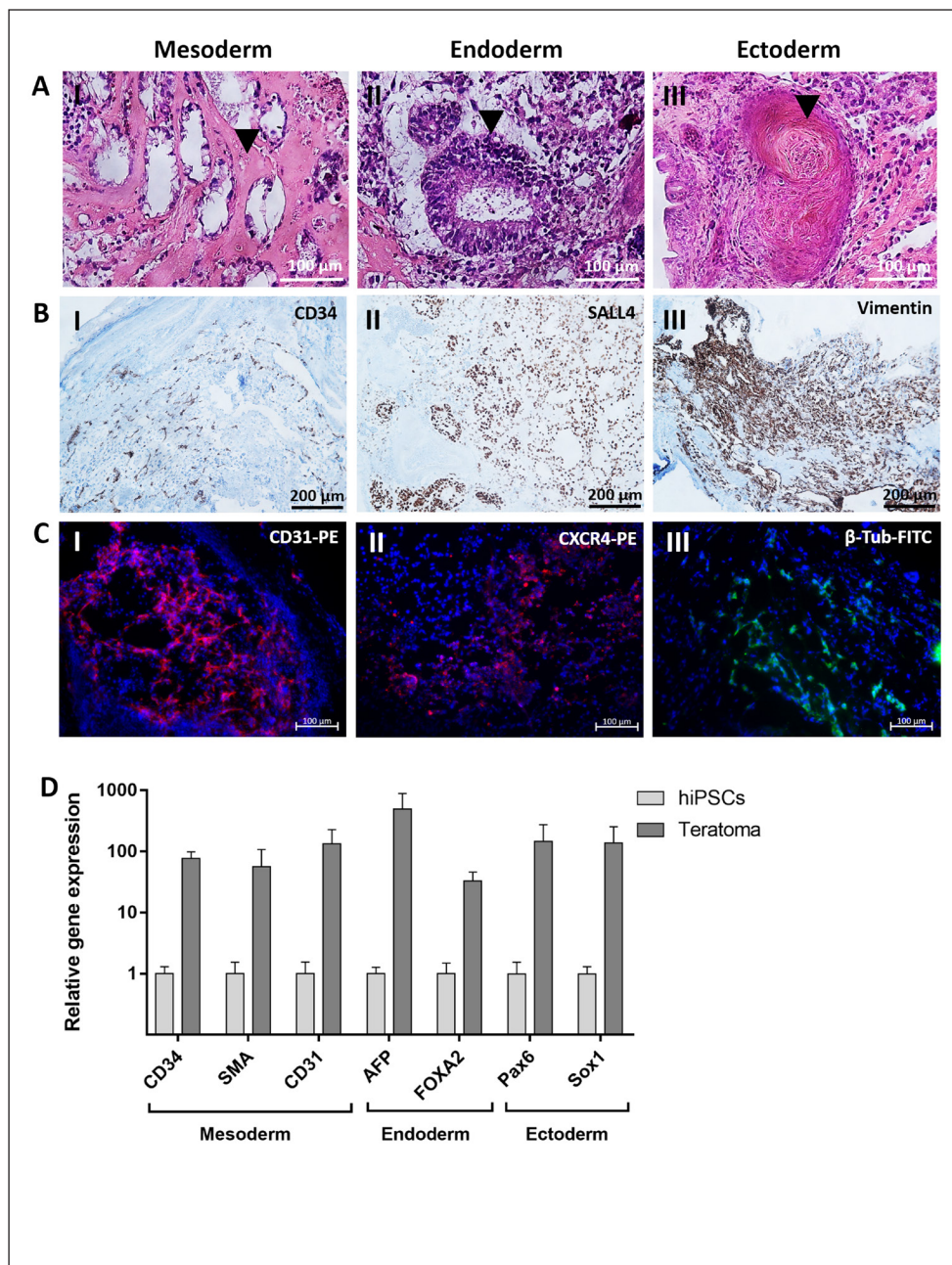


**Fig. 3: Detection of three germ layer-specific tissue types in teratoma sections**

Teratomas were generated by seeding of  $2 \times 10^6$  hiPSCs on CAMs. (A) Representative microscopic images of teratoma sections stained with H&E showing hiPSC-derived tissues of all three germ layers. Mesoderm: (I) bone-like tissue; endoderm: (II) primitive gut-like epithelium; ectoderm: (III) squamous epithelium. The arrows indicate the described germ layer-specific structures. These images are taken from two teratomas. (B) Representative microscopic images of immunohistochemical staining using antibodies against (I) CD34, (II) SALL4 and (III) vimentin. Antibody-stained tissue structures are brown; sections were counterstained with hematoxylin. These images are taken from two teratomas. (C) Representative immunofluorescence images of teratoma sections stained with (I) PE-mouse anti-human-CD31, (II) PE-mouse anti-human CXCR4 or (III) Alexa Fluor<sup>®</sup> 488-mouse anti-human  $\beta$ -tubulin antibodies. These images are taken from three teratomas. (D) qRT-PCR expression analysis of CD34, SMA, CD31, AFP, FOXA2, Pax6 and Sox1 transcripts in teratomas generated from  $2 \times 10^6$  hiPSCs. mRNA levels were normalized to GAPDH mRNA levels. Results are shown relative to hiPSCs cultivated in cell culture flask as mean + SEM (n = 3)

To further prove the functionality of the CAM model, the teratoma formation potential of two other hiPSC lines, which were generated in our laboratory by reprogramming of NuFFs or JPCs, was assessed by seeding of  $2 \times 10^6$  cells on CAM. The H&E staining of the explanted teratomas, which were generated from NuFF-derived (Fig. 4A) or JPC-derived (Fig. 4B) hiPSCs, demonstrated tri-lineage differentiation potential similar to that of hiPSC derived from RECs (Fig. 3). Differentiation into mesodermal tissue was demonstrated by the presence of bone-like structures (Fig. 4A I) and adipose tissue (Fig. 4B I). Furthermore, gut-like epithelium showing endodermal differentiation (Fig. 4A II,

4B II) and squamous epithelium showing ectodermal differentiation (Fig. 4A III, 4B III) were detected.

## 4 Discussion

Patient-specific hiPSCs offer the possibility to regenerate destroyed cell types and tissues for personalized treatment. After the generation of hiPSCs and their differentiation, an extensive characterization of the cells including confirmation of their pluripotency is required. Typically, cells are implanted in immuno-



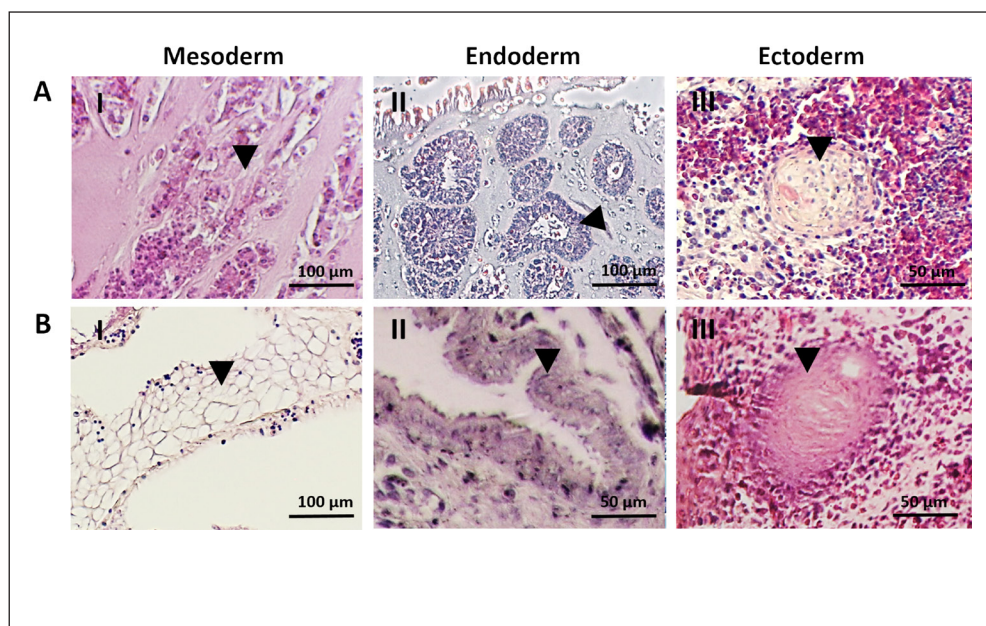


**Fig. 4: Detection of the three germ layer-specific tissue types in teratoma sections generated from NuFF- or JPC-derived hiPSCs**

Representative microscopic images of H&E stained teratoma sections of (A) NuFF-derived hiPSCs: mesoderm: (I) bone-like tissue; endoderm: (II) primitive gut-like epithelium; ectoderm: (III) squamous epithelium, and (B) JPC-derived hiPSCs: mesoderm: (I) adipose tissue; endoderm: (II) primitive gut-like epithelium; ectoderm: (III) squamous epithelium. The arrows indicate the described germ layer-specific structures. These images are taken from three teratomas, respectively.

deficient mice to demonstrate the ability of newly created hiPSCs to differentiate into all cell types of the three germ layers, i.e., mesoderm, endoderm, and ectoderm (Nelakanti et al., 2015). In this study, we tested the applicability of the CAM assay as a new *in vivo* model for the evaluation of the pluripotency of hiPSCs to reduce animal suffering.

Commonly, subcutaneous (Cao et al., 2007), intramuscular (Lee et al., 2009), intramyocardial (Cao et al., 2006), or sub-renal capsule implantation of hiPSCs is performed into 15 to 20 immunodeficient mice aged 6 to 10 weeks. The animals are maintained for a period of approximately 4 to 6 weeks to allow the growth of the implanted cells and teratoma formation (Nelakanti et al., 2015; Aldahmash et al., 2013). If the cells are transplanted subcutaneously or intraperitoneally, easily palpable teratomas are formed around 6 weeks post-injection (Zhang et al., 2008). The teratomas can be measured using the traditional caliper method (Hentze et al., 2009). Mice should be sacrificed before the teratoma is larger than 1 cm<sup>3</sup> or earlier if the dimension reached impairs the animal's behavior, motility or food and water intake due to pain or distress (Nelakanti et al., 2015). The composition of the explanted teratoma is then analyzed using histological and immunohistochemical staining.

Using the established CAM assay, the incubation of implanted hiPSCs for 9 days was sufficient to form characteristic tissue structures of all three germ layers. Thus, the established CAM model is cost-effective and far less time-consuming than the mouse model. Moreover, since the CAM is not innervated, it allows the growth of xenografts without pain or impairment of the embryo (Kunz et al., 2019). The highly vascularized CAM efficiently supports the growth of the teratoma. Furthermore, the immaturity of the chicken embryo's immune system enables the use of cells from different species (Deryugina and Quigley, 2008) as the seeded cells are not rejected.

Although the established CAM assay-based method has several advantages over the *in vivo* mouse teratoma assay, it also has some limitations. Teratoma formation on CAM can only be performed for 9-10 days after the application of hiPSCs, as the chick hatches 21 days after incubation. In contrast, in mice the incubation period can be extended to increase the size or tissue maturation of the teratoma if the animal's behavior is not negatively affected. In a further study, kinetic trajectories showed that around 37 days are required to see and measure the size of the teratoma externally (McDonald et al., 2020). Thus, we assume that the tissue structures formed in teratomas on CAM are less mature than those in mice.

However, the established CAM assay is clearly appropriate to demonstrate the tri-lineage differentiation capability of the generated hiPSCs. The robustness of the established CAM assay has been demonstrated by the successful generation of teratomas after the application of hiPSC lines generated from NuFFs or JPCs in addition to hiPSCs derived from RECs. The tri-lineage differentiation was successfully demonstrated with all three hiPSC lines. RECs seeded on CAM did not cause teratoma formation.

The Matrigel used to apply the hiPSCs to CAM is obtained from the murine Engelbreth-Holm-Swarm (EHS) tumor. Therefore, replacing Matrigel by synthetic hydrogels, such as polymers and scaffolds based on polyacrylamide and polyethylene glycol (PEG) (Aisenbrey and Murphy, 2020), will further reduce and prevent pain and suffering of animals in the future.

To test the influence of inoculated cell numbers on teratoma formation, different numbers of hiPSCs were seeded on CAM. The increase of the cell number from  $0.5 \times 10^6$  to  $2 \times 10^6$  hiPSCs led to a higher teratoma formation efficiency (30% versus 70%). The further increase of hiPSC number to  $4 \times 10^6$  cells resulted in teratoma formation on all CAMs. However,  $2 \times 10^6$  hiPSCs were sufficient to obtain teratomas containing

cells of all three germ layers. Thus, we recommend using  $2 \times 10^6$  or more hiPSCs for the teratoma analysis. In immunodeficient mice, usually,  $1 \times 10^6$  cells are used per injection, and it has been shown that injections of 2 or  $4 \times 10^6$  hiPSCs can increase the chances of successful teratoma formation in mice (Nelakanti et al., 2015).

Cells of all three germ layers were detected within the formed teratoma from  $2 \times 10^6$  hiPSCs. The presence of endoderm, mesoderm, and ectoderm tissue cell types was detected using specific antibodies as well as by detection of gene expression using qRT-PCR. In addition to using the established CAM model to analyze the pluripotency of hiPSCs, it can also be applied to determine whether unwanted hiPSCs remain in the differentiated cells. The implantation of remaining, not fully differentiated hiPSCs can lead to the formation of teratomas and must be avoided for clinical use. Thus, the CAM assay also can be applied to analyze the safety of hiPSC-derived cell types and the complete differentiation of hiPSCs into somatic cells.

## 5 Conclusion

In this study, an alternative *in vivo* model was established and tested to evaluate the pluripotency of newly generated hiPSC lines within 9 days. The CAM model is a valuable method to bridge the gap between *in vitro* cell culture and *in vivo* animal experiments. In contrast to the immunodeficient mouse model, it is simple, inexpensive, and time-saving. The application of this CAM assay can reduce the number of required animals and their suffering. Besides the pluripotency evaluation of the reprogrammed cells, the CAM assay can be also applied to test the safety of differentiated cells from hiPSCs.

## References

- Aisenbrey, E. A. and Murphy, W. L. (2020). Synthetic alternatives to matrigel. *Nat Rev Mater* 5, 539-551. doi:10.1038/s41578-020-0199-8
- Aldahmash, A., Atteya, M., Elsafadi, M. et al. (2013). Teratoma formation in immunocompetent mice after syngeneic and allogeneic implantation of germline capable mouse embryonic stem cells. *Asian Pac J Cancer Prev* 14, 5705-5711. doi:10.7314/apjcp.2013.14.10.5705
- Buhr, C. R., Wiesmann, N., Tanner, R. C. et al. (2020). The chorioallantoic membrane assay in nanotoxicological research – An alternative for *in vivo* experimentation. *Nanomaterials (Basel)* 10, 2328. doi:10.3390/nano10122328
- Buta, C., David, R., Dressel, R. et al. (2013). Reconsidering pluripotency tests: Do we still need teratoma assays? *Stem Cell Res* 11, 552-562. doi:10.1016/j.scr.2013.03.001
- Cao, F., Lin, S., Xie, X. et al. (2006). *In vivo* visualization of embryonic stem cell survival, proliferation, and migration after cardiac delivery. *Circulation* 113, 1005-1014. doi:10.1161/circulationaha.105.588954
- Cao, F., van der Bogt, K. E., Sadrzadeh, A. et al. (2007). Spatial and temporal kinetics of teratoma formation from murine embryonic stem cell transplantation. *Stem Cells Dev* 16, 883-891. doi:10.1089/scd.2007.0160
- Ciešlar-Pobuda, A., Knoflach, V., Rinh, M. V. et al. (2017). Transdifferentiation and reprogramming: Overview of the processes, their similarities and differences. *Biochim Biophys Acta Mol Cell Res* 1864, 1359-1369. doi:10.1016/j.bbamcr.2017.04.017
- DeBord, L. C., Pathak, R. R., Villaneuva, M. et al. (2018). The chick chorioallantoic membrane (CAM) as a versatile patient-derived xenograft (PDX) platform for precision medicine and preclinical research. *Am J Cancer Res* 8, 1642-1660.
- Deryugina, E. I. and Quigley, J. P. (2008). Chick embryo chorioallantoic membrane model systems to study and visualize human tumor cell metastasis. *Histochem Cell Biol* 130, 1119-1130. doi:10.1007/s00418-008-0536-2
- Dexter, D. L., Lee, E. S., DeFusco, D. J. et al. (1983). Selection of metastatic variants from heterogeneous tumor cell lines using the chicken chorioallantoic membrane and nude mouse. *Cancer Res* 43, 1733-1740.
- Dohle, D. S., Pasa, S. D., Gustmann, S. et al. (2009). Chick ex ovo culture and ex ovo CAM assay: How it really works. *J Vis Exp*, e1620. doi:10.3791/1620
- Durupt, F., Koppers-Lalic, D., Balme, B. et al. (2012). The chicken chorioallantoic membrane tumor assay as model for qualitative testing of oncolytic adenoviruses. *Cancer Gene Ther* 19, 58-68. doi:10.1038/cgt.2011.68
- Gilleron, L., Coecke, S., Sysmans, M. et al. (1996). Evaluation of a modified HET-CAM assay as a screening test for eye irritancy. *Toxicol In Vitro* 10, 431-446. doi:10.1016/0887-2333(96)00021-5
- Hentze, H., Soong, P. L., Wang, S. T. et al. (2009). Teratoma formation by human embryonic stem cells: Evaluation of essential parameters for future safety studies. *Stem Cell Res* 2, 198-210. doi:10.1016/j.scr.2009.02.002
- Kaji, K., Norrby, K., Paca, A. et al. (2009). Virus-free induction of pluripotency and subsequent excision of reprogramming factors. *Nature* 458, 771-775. doi:10.1038/nature07864
- Kibbe, W. A. (2007). OligoCalc: An online oligonucleotide properties calculator. *Nucleic Acids Res* 35, W43-46. doi:10.1093/nar/gkm234
- Kunz, P., Schenker, A., Sahr, H. et al. (2019). Optimization of the chicken chorioallantoic membrane assay as reliable *in vivo* model for the analysis of osteosarcoma. *PLoS One* 14, e0215312. doi:10.1371/journal.pone.0215312
- Kunzi-Rapp, K., Genze, F., Kufer, R. et al. (2001). Chorioallantoic membrane assay: Vascularized 3-dimensional cell culture system for human prostate cancer cells as an animal substitute model. *J Urol* 166, 1502-1507. doi:10.1016/s0022-5347(05)65820-x
- Lee, A. S., Tang, C., Cao, F. et al. (2009). Effects of cell number on teratoma formation by human embryonic stem cells. *Cell Cycle* 8, 2608-2612. doi:10.4161/cc.8.16.9353
- Li, M., Pathak, R. R., Lopez-Rivera, E. et al. (2015). The *in ovo* chick chorioallantoic membrane (CAM) assay as an efficient xenograft model of hepatocellular carcinoma. *J Vis Exp*, e52411. doi:10.3791/52411





- McDonald, D., Wu, Y., Dailamy, A. et al. (2020). Defining the teratoma as a model for multi-lineage human development. *Cell* 183, 1402-1419 e1418. doi:10.1016/j.cell.2020.10.018
- Moreno-Jimenez, I., Hulsart-Billstrom, G., Lanham, S. A. et al. (2016). The chorioallantoic membrane (CAM) assay for the study of human bone regeneration: A refinement animal model for tissue engineering. *Sci Rep* 6, 32168. doi:10.1038/srep32168
- Naik, M., Brahma, P. and Dixit, M. (2018). A cost-effective and efficient chick ex-ovo cam assay protocol to assess angiogenesis. *Methods Protoc* 1, 19. doi:10.3390/mps1020019
- Nelakanti, R. V., Kooreman, N. G. and Wu, J. C. (2015). Teratoma formation: A tool for monitoring pluripotency in stem cell research. *Curr Protoc Stem Cell Biol* 32, 4A.8.1-17. doi:10.1002/9780470151808.sc04a08s32
- Petrovova, E., Giretova, M., Kvasilova, A. et al. (2019). Preclinical alternative model for analysis of porous scaffold biocompatibility in bone tissue engineering. *ALTEX* 36, 121-130. doi:10.14573/altex.1807241
- Rabinovich, P. M. and Weissman, S. M. (2013). Cell engineering with synthetic messenger RNA. *Methods Mol Biol* 969, 3-28. doi:10.1007/978-1-62703-260-5\_1
- Rovithi, M., Avan, A., Funel, N. et al. (2017). Development of bioluminescent chick chorioallantoic membrane (CAM) models for primary pancreatic cancer cells: A platform for drug testing. *Sci Rep* 7, 44686. doi:10.1038/srep44686
- Steinle, H., Behring, A., Schlensak, C. et al. (2017). Concise review: Application of in vitro transcribed messenger RNA for cellular engineering and reprogramming: Progress and challenges. *Stem Cells* 35, 68-79. doi:10.1002/stem.2402
- Steinle, H., Golombek, S., Behring, A. et al. (2018). Improving the angiogenic potential of EPCs via engineering with synthetic modified mRNAs. *Mol Ther Nucleic Acids* 13, 387-398. doi:10.1016/j.omtn.2018.09.005
- Steinle, H., Weber, M., Behring, A. et al. (2019a). Generation of iPSCs by nonintegrative RNA-based reprogramming techniques: Benefits of self-replicating RNA versus synthetic mRNA. *Stem Cells Int* 2019, 7641767. doi:10.1155/2019/7641767
- Steinle, H., Weber, M., Behring, A. et al. (2019b). Reprogramming of urine-derived renal epithelial cells into iPSCs using srRNA and consecutive differentiation into beating cardiomyocytes. *Mol Ther Nucleic Acids* 17, 907-921. doi:10.1016/j.omtn.2019.07.016
- Takahashi, K. and Yamanaka, S. (2006). Induction of pluripotent stem cells from mouse embryonic and adult fibroblast cultures by defined factors. *Cell* 126, 663-676. doi:10.1016/j.cell.2006.07.024
- Takahashi, K., Tanabe, K., Ohnuki, M. et al. (2007). Induction of pluripotent stem cells from adult human fibroblasts by defined factors. *Cell* 131, 861-872. doi:10.1016/j.cell.2007.11.019
- Warren, L., Manos, P. D., Ahfeldt, T. et al. (2010). Highly efficient reprogramming to pluripotency and directed differentiation of human cells with synthetic modified mRNA. *Cell Stem Cell* 7, 618-630. doi:10.1016/j.stem.2010.08.012
- Winter, G., Koch, A. B. F., Löffler, J. et al. (2020). Multi-modal PET and MR imaging in the hen's egg test-chorioallantoic membrane (HET-CAM) model for initial in vivo testing of target-specific radioligands. *Cancers (Basel)* 12, 1248. doi:10.3390/cancers12051248
- Ye, J., Coulouris, G., Zaretskaya, I. et al. (2012). Primer-blast: A tool to design target-specific primers for polymerase chain reaction. *BMC Bioinformatics* 13, 134. doi:10.1186/1471-2105-13-134
- Ying, Y., Xingfen, Y., Wengai, Z. et al. (2010). Combined in vitro tests as an alternative to in vivo eye irritation tests. *Altern Lab Anim* 38, 303-314. doi:10.1177/026119291003800413
- Yu, J., Hu, K., Smuga-Otto, K. et al. (2009). Human induced pluripotent stem cells free of vector and transgene sequences. *Science* 324, 797-801. doi:10.1126/science.1172482
- Zhang, W. Y., de Almeida, P. E. and Wu, J. C. (2008). Teratoma formation: A tool for monitoring pluripotency in stem cell research. In *StemBook*. Cambridge (MA). doi:10.3824/stembook.1.53.1

### Conflict of interest

All authors declare no competing financial interests relevant to the submitted work.

### Acknowledgements

For antibody staining, the authors would like to thank Dr Irene Gonzalez Menendez and Prof. Dr Leticia Quintanilla de Fend at the Institute of Pathology, University Hospital & Comprehensive Cancer Center, University of Tübingen. We acknowledge support by the German Research Foundation (Deutsche Forschungsgemeinschaft; DFG) through AV 133/7-1 and the Open Access Publishing Fund of University of Tübingen.